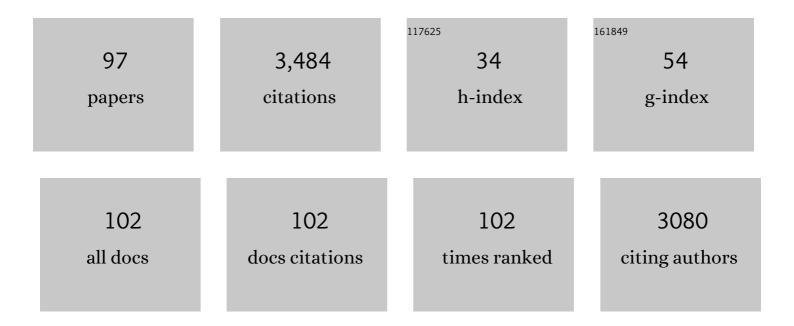
## Ingo Zebger

List of Publications by Year in descending order

Source: https://exaly.com/author-pdf/5436732/publications.pdf Version: 2024-02-01



INCO 7ERCER

#	Article	IF	CITATIONS
1	Unusual structures and unknown roles of FeS clusters in metalloenzymes seen from a resonance Raman spectroscopic perspective. Coordination Chemistry Reviews, 2022, 452, 214287.	18.8	16
2	An Intermetallic CaFe <sub>6</sub> Ge <sub>6</sub> Approach to Unprecedented Caâ^'Feâ^'O Electrocatalyst for Efficient Alkaline Oxygen Evolution Reaction. ChemCatChem, 2022, 14, .	3.7	10
3	High-Yield Production of Catalytically Active Regulatory [NiFe]-Hydrogenase From Cupriavidus necator in Escherichia coli. Frontiers in Microbiology, 2022, 13, 894375.	3.5	5
4	Electrografted Interfaces on Metal Oxide Electrodes for Enzyme Immobilization and Bioelectrocatalysis. ChemElectroChem, 2021, 8, 1329-1336.	3.4	6
5	Simple and robust: The claims of protein sensing by molecularly imprinted polymers. Sensors and Actuators B: Chemical, 2021, 330, 129369.	7.8	41
6	Ein neuer Aufbau zur Untersuchung der Struktur und Funktion von solvatisierten, lyophilisierten und kristallinen Metalloenzymen – veranschaulicht anhand von [NiFe]â€Hydrogenasen. Angewandte Chemie, 2021, 133, 15988-15996.	2.0	0
7	Exploring Structure and Function of Redox Intermediates in [NiFe]â€Hydrogenases by an Advanced Experimental Approach for Solvated, Lyophilized and Crystallized Metalloenzymes. Angewandte Chemie - International Edition, 2021, 60, 15854-15862.	13.8	15
8	Two ligand-binding sites in CO-reducing V nitrogenase reveal a general mechanistic principle. Science Advances, 2021, 7, .	10.3	33
9	Insights in electrosynthesis, target binding, and stability of peptide-imprinted polymer nanofilms. Electrochimica Acta, 2021, 381, 138236.	5.2	11
10	"Out of Pocket―Protein Binding—A Dilemma of Epitope Imprinted Polymers Revealed for Human Hemoglobin. Chemosensors, 2021, 9, 128.	3.6	13
11	Frontispiz: Ein neuer Aufbau zur Untersuchung der Struktur und Funktion von solvatisierten, lyophilisierten und kristallinen Metalloenzymen – veranschaulicht anhand von [NiFe]â€Hydrogenasen. Angewandte Chemie, 2021, 133, .	2.0	0
12	Frontispiece: Exploring Structure and Function of Redox Intermediates in [NiFe]â€Hydrogenases by an Advanced Experimental Approach for Solvated, Lyophilized and Crystallized Metalloenzymes. Angewandte Chemie - International Edition, 2021, 60, .	13.8	0
13	Molecular Details on Multiple Cofactor Containing Redox Metalloproteins Revealed by Infrared and Resonance Raman Spectroscopies. Molecules, 2021, 26, 4852.	3.8	1
14	Local Electric Field Changes during the Photoconversion of the Bathy Phytochrome Agp2. Biochemistry, 2021, 60, 2967-2977.	2.5	10
15	Hydroxy-bridged resting states of a [NiFe]-hydrogenase unraveled by cryogenic vibrational spectroscopy and DFT computations. Chemical Science, 2021, 12, 2189-2197.	7.4	17
16	Host–Guest Chemistry Meets Electrocatalysis: Cucurbit[6]uril on a Au Surface as a Hybrid System in CO <sub>2</sub> Reduction. ACS Catalysis, 2020, 10, 751-761.	11.2	43
17	<i>In Vitro</i> Assembly as a Tool to Investigate Catalytic Intermediates of [NiFe]-Hydrogenase. ACS Catalysis, 2020, 10, 13890-13894.	11.2	13
18	Understanding the formation of bulk- and surface-active layered (oxy)hydroxides for water oxidation starting from a cobalt selenite precursor. Energy and Environmental Science, 2020, 13, 3607-3619.	30.8	77

#	Article	IF	CITATIONS
19	A soft molecular 2Fe–2As precursor approach to the synthesis of nanostructured FeAs for efficient electrocatalytic water oxidation. Chemical Science, 2020, 11, 11834-11842.	7.4	30
20	Caught in the H inact : Crystal Structure and Spectroscopy Reveal a Sulfur Bound to the Active Site of an O 2 â€stable State of [FeFe] Hydrogenase. Angewandte Chemie - International Edition, 2020, 59, 16786-16794.	13.8	40
21	Kristallstruktur und Spektroskopie offenbaren einen Schwefelâ€Liganden am aktiven Zentrum einer O 2 â€stabilen [FeFe]â€Hydrogenase. Angewandte Chemie, 2020, 132, 16930.	2.0	6
22	Shedding Light on Proton and Electron Dynamics in [FeFe] Hydrogenases. Journal of the American Chemical Society, 2020, 142, 5493-5497.	13.7	38
23	The large subunit of the regulatory [NiFe]-hydrogenase fromRalstonia eutropha– a minimal hydrogenase?. Chemical Science, 2020, 11, 5453-5465.	7.4	20
24	Xâ€ray Crystallography and Vibrational Spectroscopy Reveal the Key Determinants of Biocatalytic Dihydrogen Cycling by [NiFe] Hydrogenases. Angewandte Chemie - International Edition, 2019, 58, 18710-18714.	13.8	32
25	Xâ€ray Crystallography and Vibrational Spectroscopy Reveal the Key Determinants of Biocatalytic Dihydrogen Cycling by [NiFe] Hydrogenases. Angewandte Chemie, 2019, 131, 18883-18887.	2.0	6
26	Comparison of molybdenum and rhenium oxo bis-pyrazine-dithiolene complexes – in search of an alternative metal centre for molybdenum cofactor models. Dalton Transactions, 2019, 48, 2701-2714.	3.3	10
27	Electrosynthesized MIPs for transferrin: Plastibodies or nano-filters?. Biosensors and Bioelectronics, 2018, 105, 29-35.	10.1	38
28	Catalytic Activity and Proton Translocation of Reconstituted Respiratory Complex I Monitored by Surface-Enhanced Infrared Absorption Spectroscopy. Langmuir, 2018, 34, 5703-5711.	3.5	13
29	Enzymatic and spectroscopic properties of a thermostable [NiFe]‑hydrogenase performing H2-driven NAD+-reduction in the presence of O2. Biochimica Et Biophysica Acta - Bioenergetics, 2018, 1859, 8-18.	1.0	14
30	In Situ Spectroelectrochemical Studies into the Formation and Stability of Robust Diazonium-Derived Interfaces on Gold Electrodes for the Immobilization of an Oxygen-Tolerant Hydrogenase. ACS Applied Materials & Interfaces, 2018, 10, 23380-23391.	8.0	23
31	Robust electrografted interfaces on metal oxides for electrocatalysis – an <i>in situ</i> spectroelectrochemical study. Journal of Materials Chemistry A, 2018, 6, 15200-15212.	10.3	33
32	O <sub>2</sub> -Tolerant H <sub>2</sub> Activation by an Isolated Large Subunit of a [NiFe] Hydrogenase. Biochemistry, 2018, 57, 5339-5349.	2.5	16
33	Solar Water Splitting with a Hydrogenase Integrated in Photoelectrochemical Tandem Cells. Angewandte Chemie - International Edition, 2018, 57, 10595-10599.	13.8	93
34	An Sâ€Oxygenated [NiFe] Complex Modelling Sulfenate Intermediates of an O <sub>2</sub> â€₹olerant Hydrogenase. Angewandte Chemie - International Edition, 2017, 56, 2208-2211.	13.8	21
35	Characterization of Frex as an NADH sensor for in vivo applications in the presence of NAD+ and at various pH values. Photosynthesis Research, 2017, 133, 305-315.	2.9	9
36	Carbon Monoxide Dehydrogenase Reduces Cyanate to Cyanide. Angewandte Chemie - International Edition, 2017, 56, 7398-7401.	13.8	10

#	Article	IF	CITATIONS
37	Determination of the Local Electric Field at Au/SAM Interfaces Using the Vibrational Stark Effect. Journal of Physical Chemistry C, 2017, 121, 22274-22285.	3.1	41
38	Tuning Product Selectivity for Aqueous CO <sub>2</sub> Reduction with a Mn(bipyridine)-pyrene Catalyst Immobilized on a Carbon Nanotube Electrode. Journal of the American Chemical Society, 2017, 139, 14425-14435.	13.7	185
39	Investigation of the NADH/NAD + ratio in Ralstonia eutropha using the fluorescence reporter protein Peredox. Biochimica Et Biophysica Acta - Bioenergetics, 2017, 1858, 86-94.	1.0	19
40	CO synthesized from the central one-carbon pool as source for the iron carbonyl in O2-tolerant [NiFe]-hydrogenase. Proceedings of the National Academy of Sciences of the United States of America, 2016, 113, 14722-14726.	7.1	28
41	Domain motions and electron transfer dynamics in 2Fe-superoxide reductase. Physical Chemistry Chemical Physics, 2016, 18, 23053-23066.	2.8	5
42	When the inhibitor tells more than the substrate: the cyanide-bound state of a carbon monoxide dehydrogenase. Chemical Science, 2016, 7, 3162-3171.	7.4	22
43	Spectroscopic Observation of Calciumâ€Induced Reorientation of Cellobiose Dehydrogenase Immobilized on Electrodes and its Effect on Electrocatalytic Activity. ChemPhysChem, 2015, 16, 1960-1968.	2.1	31
44	Orientation-Controlled Electrocatalytic Efficiency of an Adsorbed Oxygen-Tolerant Hydrogenase. PLoS ONE, 2015, 10, e0143101.	2.5	29
45	Nuclear resonance vibrational spectroscopy reveals the FeS cluster composition and active site vibrational properties of an O <sub>2</sub> -tolerant NAD <sup>+</sup> -reducing [NiFe] hydrogenase. Chemical Science, 2015, 6, 1055-1060.	7.4	27
46	Impact of the Iron–Sulfur Cluster Proximal to the Active Site on the Catalytic Function of an O <sub>2</sub> -Tolerant NAD <sup>+</sup> -Reducing [NiFe]-Hydrogenase. Biochemistry, 2015, 54, 389-403.	2.5	16
47	Reversible Active Site Sulfoxygenation Can Explain the Oxygen Tolerance of a NAD <sup>+</sup> -Reducing [NiFe] Hydrogenase and Its Unusual Infrared Spectroscopic Properties. Journal of the American Chemical Society, 2015, 137, 2555-2564.	13.7	35
48	Resonance Raman Spectroscopic Analysis of the [NiFe] Active Site and the Proximal [4Fe-3S] Cluster of an O <sub>2</sub> -Tolerant Membrane-Bound Hydrogenase in the Crystalline State. Journal of Physical Chemistry B, 2015, 119, 13785-13796.	2.6	30
49	Electrochemical and Infrared Spectroscopic Studies Provide Insight into Reactions of the NiFe Regulatory Hydrogenase from <i>Ralstonia eutropha</i> with O <sub>2</sub> and CO. Journal of Physical Chemistry B, 2015, 119, 13807-13815.	2.6	30
50	Rubredoxin-related Maturation Factor Guarantees Metal Cofactor Integrity during Aerobic Biosynthesis of Membrane-bound [NiFe] Hydrogenase. Journal of Biological Chemistry, 2014, 289, 7982-7993.	3.4	10
51	Reversible [4Fe-3S] cluster morphing in an O2-tolerant [NiFe] hydrogenase. Nature Chemical Biology, 2014, 10, 378-385.	8.0	85
52	Resonance Raman Spectroscopy on [NiFe] Hydrogenase Provides Structural Insights into Catalytic Intermediates and Reactions. Journal of the American Chemical Society, 2014, 136, 9870-9873.	13.7	60
53	Metal-induced histidine deprotonation in biocatalysis? Experimental and theoretical insights into superoxide reductase. RSC Advances, 2014, 4, 54091-54095.	3.6	10
54	Effect of the Protonation Degree of a Self-Assembled Monolayer on the Immobilization Dynamics of a [NiFe] Hydrogenase. Langmuir, 2013, 29, 673-682.	3.5	22

#	Article	IF	CITATIONS
55	Combining Spectroscopy and Theory to Evaluate Structural Models of Metalloenzymes: A Case Study on the Soluble [NiFe] Hydrogenase from <i>Ralstonia eutropha</i> . ChemPhysChem, 2013, 14, 185-191.	2.1	8
56	Resonance Raman Spectroscopy as a Tool to Monitor the Active Site of Hydrogenases. Angewandte Chemie - International Edition, 2013, 52, 5162-5165.	13.8	53
57	A Universal Scaffold for Synthesis of the Fe(CN)2(CO) Moiety of [NiFe] Hydrogenase. Journal of Biological Chemistry, 2012, 287, 38845-38853.	3.4	49
58	Vibrational Stark Effect of the Electric-Field Reporter 4-Mercaptobenzonitrile as a Tool for Investigating Electrostatics at Electrode/SAM/Solution Interfaces. International Journal of Molecular Sciences, 2012, 13, 7466-7482.	4.1	59
59	Revealing the Absolute Configuration of the CO and CN <sup>â^'</sup> Ligands at the Active Site of a [NiFe] Hydrogenase. ChemPhysChem, 2012, 13, 3852-3856.	2.1	20
60	Analyzing the catalytic processes of immobilized redox enzymes by vibrational spectroscopies. IUBMB Life, 2012, 64, 455-464.	3.4	33
61	Insights into the structure of the active site of the O2-tolerant membrane bound [NiFe] hydrogenase of R. eutropha H16 by molecular modelling. Physical Chemistry Chemical Physics, 2011, 13, 16146.	2.8	16
62	[NiFe] and [FeS] Cofactors in the Membrane-Bound Hydrogenase of <i>Ralstonia eutropha</i> Investigated by X-ray Absorption Spectroscopy: Insights into O <sub>2</sub> -Tolerant H <sub>2</sub> Cleavage. Biochemistry, 2011, 50, 5858-5869.	2.5	33
63	Surfaceâ€enhanced vibrational spectroscopy for probing transient interactions of proteins with biomimetic interfaces: electric field effects on structure, dynamics and function of cytochrome <i>c</i> . FEBS Journal, 2011, 278, 1382-1390.	4.7	64
64	A unique iron-sulfur cluster is crucial for oxygen tolerance of a [NiFe]-hydrogenase. Nature Chemical Biology, 2011, 7, 310-318.	8.0	225
65	Role of the HoxZ Subunit in the Electron Transfer Pathway of the Membrane-Bound [NiFe]-Hydrogenase from <i>Ralstonia eutropha</i> Immobilized on Electrodes. Journal of Physical Chemistry B, 2011, 115, 10368-10374.	2.6	39
66	The Hydrogenase Subcomplex of the NAD <sup>+</sup> â€Reducing [NiFe] Hydrogenase from <i>Ralstonia eutropha</i> – Insights into Catalysis and Redox Interconversions. European Journal of Inorganic Chemistry, 2011, 2011, 1067-1079.	2.0	47
67	SEIRA Spectroscopy of the Electrochemical Activation of an Immobilized [NiFe] Hydrogenase under Turnover and Nonâ€7urnover Conditions. Angewandte Chemie - International Edition, 2011, 50, 2632-2634.	13.8	48
68	Probing the Origin of the Metabolic Precursor of the CO Ligand in the Catalytic Center of [NiFe] Hydrogenase. Journal of Biological Chemistry, 2011, 286, 44937-44944.	3.4	30
69	Impact of Amino Acid Substitutions near the Catalytic Site on the Spectral Properties of an O <sub>2</sub> â€Tolerant Membraneâ€Bound [NiFe] Hydrogenase. ChemPhysChem, 2010, 11, 1215-1224.	2.1	10
70	Protein–Protein Complex Formation Affects the Ni–Fe and Fe–S Centers in the H <sub>2</sub> ‧ensing Regulatory Hydrogenase from <i>Ralstonia eutropha</i> H16. ChemPhysChem, 2010, 11, 1297-1306.	2.1	11
71	Probing the Active Site of an O <sub>2</sub> â€Tolerant NAD <sup>+</sup> â€Reducing [NiFe]â€Hydrogenase from <i>Ralstonia eutropha</i> H16 by Inâ€Situ EPR and FTIR Spectroscopy. Angewandte Chemie - International Edition, 2010, 49, 8026-8029.	13.8	65
72	Spectroscopic Insights into the Oxygen-tolerant Membrane-associated [NiFe] Hydrogenase of Ralstonia eutropha H16. Journal of Biological Chemistry, 2009, 284, 16264-16276.	3.4	102

#	Article	IF	CITATIONS
73	Overexpression, Isolation, and Spectroscopic Characterization of the Bidirectional [NiFe] Hydrogenase from Synechocystis sp. PCC 6803. Journal of Biological Chemistry, 2009, 284, 36462-36472.	3.4	54
74	Concerted Action of Two Novel Auxiliary Proteins in Assembly of the Active Site in a Membrane-bound [NiFe] Hydrogenase. Journal of Biological Chemistry, 2009, 284, 2159-2168.	3.4	44
75	Monitoring Catalysis of the Membraneâ€Bound Hydrogenase from <i>Ralstonia eutropha</i> H16 by Surfaceâ€Enhanced IR Absorption Spectroscopy. Angewandte Chemie - International Edition, 2009, 48, 611-613.	13.8	46
76	Spectroelectrochemical Study of the [NiFe] Hydrogenase from Desulfovibrio vulgaris Miyazaki F in Solution and Immobilized on Biocompatible Gold Surfaces. Journal of Physical Chemistry B, 2009, 113, 15344-15351.	2.6	61
77	Redox-linked protein dynamics of cytochrome c probed by time-resolved surface enhanced infrared absorption spectroscopy. Physical Chemistry Chemical Physics, 2008, 10, 5276.	2.8	62
78	SERR-Spectroelectrochemical Study of a <i>cbb</i> <sub>3</sub> Oxygen Reductase in a Biomimetic Construct. Journal of Physical Chemistry B, 2008, 112, 16952-16959.	2.6	35
79	Application of UV/VISâ€Reflection Spectroscopy for Determination of the Oxidation State of Liquid Slags with High Fe <sup>3+</sup> â€Contents. Steel Research International, 2007, 78, 685-692.	1.8	0
80	Carbamoylphosphate serves as the source of CNâ'', but not of the intrinsic CO in the active site of the regulatory [NiFe]-hydrogenase fromRalstonia eutropha. FEBS Letters, 2007, 581, 3322-3326.	2.8	53
81	From The Cover: Electrocatalytic hydrogen oxidation by an enzyme at high carbon monoxide or oxygen levels. Proceedings of the National Academy of Sciences of the United States of America, 2005, 102, 16951-16954.	7.1	250
82	Reduction of Unusual Iron-Sulfur Clusters in the H2-sensing Regulatory Ni-Fe Hydrogenase from Ralstonia eutropha H16. Journal of Biological Chemistry, 2005, 280, 19488-19495.	3.4	42
83	Ultraviolet/visible reflection spectroscopy of molten and glassy silicates (MeOn–CaO–SiO2) and phosphates (MeOn–CaO–P2O5), Men+=Fe3+, Mn2+. Journal of Non-Crystalline Solids, 2005, 351, 3443-3457.	3.1	7
84	The structure of the Ni-Fe site in the isolated HoxC subunit of the hydrogen-sensing hydrogenase fromRalstonia eutropha. FEBS Letters, 2005, 579, 4287-4291.	2.8	26
85	Singlet Oxygen Microscope:  From Phase-Separated Polymers to Single Biological Cells. Accounts of Chemical Research, 2004, 37, 894-901.	15.6	75
86	Direct Optical Detection of Singlet Oxygen from a Single Cell¶. Photochemistry and Photobiology, 2004, 79, 319.	2.5	60
87	Structure of Liquid Slags and Ultraviolet/Visible Reflection Spectroscopy of Molten and Glassy Silicates (Fe <sub>2</sub> O <sub>3</sub> aO iO <sub>2</sub> ). Steel Research International, 2004, 75, 632-644.	1.8	1
88	Oxygen Diffusion in Copolymers of Ethylene and Norbornene. Macromolecules, 2003, 36, 7189-7198.	4.8	33
89	Singlet Oxygen Images of Heterogeneous Samples:Â Examining the Effect of Singlet Oxygen Diffusion across the Interfacial Boundary in Phase-Separated Liquids and Polymers. Langmuir, 2003, 19, 8927-8933.	3.5	40
90	Photoorientation of a Liquid-Crystalline Polyester with Azobenzene Side Groups:Â Effects of Irradiation with Linearly Polarized Red Light after Photochemical Pretreatmentâ€. Macromolecules, 2003, 36, 9373-9382.	4.8	45

#	Article	IF	CITATIONS
91	Oxygen Diffusion in Bilayer Polymer Films. Journal of Physical Chemistry B, 2003, 107, 13885-13891.	2.6	21
92	A Singlet Oxygen Image with 2.5 μm Resolution. Journal of Physical Chemistry A, 2002, 106, 8488-8490.	2.5	34
93	Ultraviolet/visible spectroscopy of molten slags and glasses (up to 1600°C). Journal of Non-Crystalline Solids, 2001, 282, 30-40.	3.1	9
94	Side-chain Liquid Crystalline Polyesters for Optical Information Storage. Polymers for Advanced Technologies, 1996, 7, 768-776.	3.2	33
95	The influence of substituents on the orientational behaviour of novel azobenzene side hain polyesters. Macromolecular Symposia, 1995, 94, 159-170.	0.7	9
96	On the explanation of the biphotonic processes in polyesters containing azobenzene moieties in the side chain. Macromolecular Rapid Communications, 1995, 16, 455-461.	3.9	46
97	Resonance Raman spectroscopic analysis of the iron–sulfur cluster redox chain of the Ralstonia eutropha membraneâ€bound [NiFe]â€hydrogenase. Journal of Raman Spectroscopy, 0, , .	2.5	4